Surface-Enhanced Raman Spectroscopic Study of Uracil. The Influence of the Surface Substrate, Surface Potential, and pH

Bernd Giese and Don McNaughton*

School of Chemistry and Centre for Biospectroscopy, Monash University, Wellington Rd, Clayton, Victoria, Australia

Received: May 24, 2001; In Final Form: October 9, 2001

The Raman and surface-enhanced Raman spectra of uracil have been recorded under a range of experimental conditions and the vibrational spectra of uracil and deprotonated uracil in the condensed phase are predicted by density functional theory (DFT) calculations at the B3LYP/6-31^{++}G(d,p) level. Solvation effects are taken into consideration in two different ways: in the context of a self-consistent reaction field of a dielectric continuum and by the explicit addition of two water molecules that can form H-bonds with the C═O and N−H moieties of uracil. On the basis of these calculations combined with normal Raman spectroscopy (NRS), two different tautomers corresponding to N1- and N3-deprotonated uracil are identified in alkaline aqueous solution, the N1-deprotonated species being slightly more common. In the SERS spectra of alkaline uracil solution in a silver sol, contributions from both tautomers are detected. The ratio of the two tautomers depends on the analyte concentration. At submonolayer concentrations (ca. 10^{-6} M) both tautomers interact with the silver surface via the respective deprotonated nitrogens adopting tilted orientations. At higher concentrations the competition for adsorption sites leads to a more upright orientation of the adsorbed species and the N3-deprotonated tautomer being favored. DFT calculations at the B3LYP/LanL2DZ level prove that N3-deprotonated uracil is stabilized more by the presence of Ag^+ ions at the metal surface than N1-deprotonated uracil. At neutral pH uracil adsorbs to the silver colloid exclusively in its N-3 deprotonated form. The interaction between uracil and an electrochemically roughened silver electrode is similar to the interaction between uracil and the silver colloid. Spectral changes caused by varying the applied electrode potential are most likely due to the inductive effect of the metal rather than a molecular reorientation at the metal surface.

Introduction

Raman spectroscopy is an invaluable tool in the study of the structure of biomolecules, including nucleic acid bases (NAB).[1−9] The application of normal Raman spectroscopy (NRS) is hampered by its poor sensitivity and by the interference of fluorescence. One way to overcome these disadvantages is through the use of surface-enhanced Raman spectroscopy (SERS).[10−13] When an analyte is adsorbed to a roughened metallic surface, fluorescence may be quenched[10] and the Raman scattering cross-section may be enhanced by up to a factor of 10^{14}.[14−16] Although the exact enhancement mechanism is not yet completely understood, there is general agreement that a combination of chemical and electromagnetic effects is at work.[11] In electromagnetic models,[17−20] enhancement results from an increase in intensity of the electromagnetic field of the incident and/or the Raman scattered light due to resonance with the surface plasmons of the SERS substrate. In chemical models,[10−13] the formation of a photoinduced charge-transfer complex between the analyte and the metal surface leads to an increase in the polarizability of the analyte. This study forms part of our investigation into the interaction of NABs with different SERS substrates.[21]

Uracil (Figure 1), like cytosine, is a pyrimidine base. It exists in RNA, but not in DNA, where it is replaced by its 5-methylated analogue, thymine. In cell processes involving RNA, such as gene expression, uracil interacts with adenine via the formation of two H-bonds. One of the carbonyl groups (O4) and one hydrogen bound to a ring nitrogen (N3) participate in the Watson−Crick interaction between adenine and uracil.

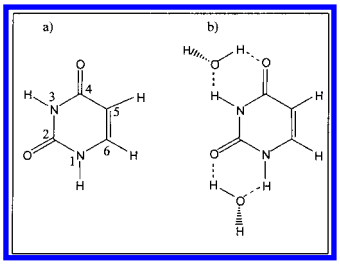

Figure 1. Atomic labeling for uracil and uracil dihydrate.

The SERS spectrum of uracil has been reported by various authors,[22−26] but the spectra obtained are quite different from one another and contrasting models for the adsorption of uracil on the surface substrate have been proposed. Suh and Moskovits[24] deduced an upright or tilted orientation of uracil on a borohydride reduced silver sol on the basis of strong SERS bands due to the CH-stretching and the ring breathing vibrations. According to the surface selection rules these bands are enhanced substantially only when an erect or tilted orientation is adopted.[27,28] These authors did not comment on what part of the molecule might interact with the metal surface. Torres and Winefordner's SERS spectrum of uracil in the same silver sol[25] differs from Suh and Moskovits'[24] with regard to both wave-

* To whom correspondence should be addressed. Address: School of Chemistry, Monash University, PO Box 23, Clayton, Vic 3800, Australia. Phone: +61 3 9905 4525. Fax: +61 3 9905 4597. E-mail: Don.McNaughton@sci.monash.edu.au.

10.1021/jp011986h CCC: $22.00
Published on Web 01/19/2002

number values and relative intensities. A comparison between the SERS spectra of uracil and 6-amino-uracil led them[25] to speculate that interaction with the metal surface might be via O4 in the case of uracil and the amino group in the case of 6-amino-uracil. Oh et al.[23] proposed that uracil adsorbed to a silver sol in its N3 deprotonated form and in a perpendicular orientation, which changed to flat as the surface charge was made more negative. Xue et al.[26] also reported adsorption of the N3 deprotonated form of uracil to a silver electrode. According to these authors the adsorption is concentration dependent changing from flat to upright as the concentration of uracil is increased. Interaction between the adsorbate and the metal surface is via the π electron system in the former case, and N3 and one or both of the carbonyl groups in the latter. Brabec and Niki[22] proposed a flat orientation for uracil on a silver electrode by transferring differential capacitance and electrocapillary measurements at a mercury electrode to the silver electrode system.

For a proper understanding of NRS and SERS spectra, a reliable assignment of all vibrational bands is essential. Together with deuteration studies, ab initio and density functional theory (DFT) methods are invaluable tools for the assignment of vibrational spectra. Due to its simple structure and planar symmetry, uracil is the most theoretically studied nucleic acid base. The vibrational spectrum of uracil has been predicted by ab initio Hartree−Fock calculations using STO-3G,[29,30] MINI-1,[30] 4-21G,[31] 6-31G(d),[32,33] and 6-31G(d,p)[34] basis sets. Electron correlation has been taken into consideration by Rush III and Peticolas,[33] who calculated the theoretical resonance Raman spectrum (RRS) of uracil at the HF and MP2 levels of theory using the 6-31G(d) basis set. Surprisingly, they found better correlation between theory and experiment for HF rather than MP2 calculations. Estrin et al.[35] employed various local density and gradient-corrected density functionals and a double-ζ plus polarization orbital basis set equivalent to the standard 6-31G-(d,p) basis set to predict the IR spectrum of uracil. The same authors later extended their study to include solvation effects[36] on the basis of Onsager's continuum solvent model.[37]

The modeling of the solvation effect was considerably improved by the pioneering work of Ghomi and co-workers.[38,39] They were the first to analyze the effect of intermolecular H-bonding on the characteristic modes arising from N−H and C═O vibrational modes by explicitly adding two water molecules. In calculations at the B3LYP level using a nonstandard double-ζ split valence basis set augmented with polarization functions at the heavy atoms and semidiffuse orbitals at those atoms directly involved in H-bonding, it was shown that H-bonding had a large effect on these vibrational modes. On the other hand an Onsager's continuum solvent model had comparably little effect. Later, Bencivienni et al.[40] investigated the influence of H-bonding on the vibrational spectrum of uracil by performing normal coordinate analysis of several uracil monohydrates and uracil dimers at the MP2 and various DFT levels using 6-31G(d) and 6-311$^+$G(d,p) basis sets. Very recently, solvation models for uracil have been further improved by the explicit addition of 1 to 7 water molecules in theoretical calculations at the MP2 level,[41] and at the B3LYP level with 6-31G*[42] and 6-31^{++}G*[43] basis sets.

Since deprotonation of uracil upon adsorption to different surface substrates has been reported by several authors, a good understanding of the Raman spectra of the uracil anions deprotonated at N1 or N3 (Figure 2) is also required for the reliable interpretation of the SERS spectra. Ilich et al.[44] considered deprotonation in their DFT study of solvated uracil.

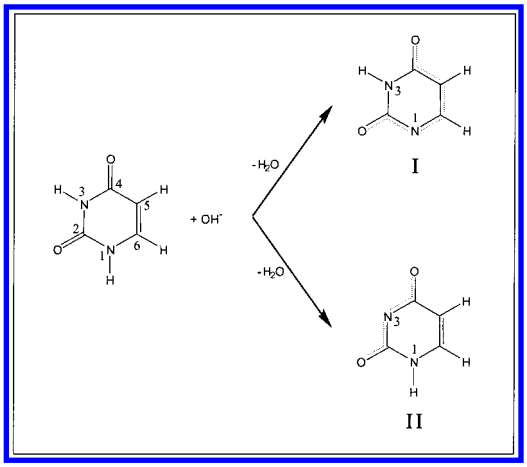

Figure 2. Deprotonation reaction of uracil.

These authors, however, used Gaussian 94 software, which only allowed them to calculate Raman intensities at the HF, but not the DFT level. Further, they only performed frequency calculations on N1 deprotonated uracil and did not consider the effects of H-bonding.

Most of the studies above were applied to the assignment of the vibrational bands in the matrix isolation IR spectrum (MI−IR) of uracil in a nitrogen or argon matrix,[29,31,32,34] or in the IR or Neutron Inelastic Scattering (NIS) spectrum of uracil in the condensed phase.[45] Only a few studies have attempted an assignment of the Raman spectrum of uracil in the condensed phase.[38,42,43] None of the DFT studies presented Raman intensities. To date Raman intensities have only been presented at the HF level with the 6-31$^+$G* basis set and without the modeling of solvation effects.[44]

Since the Raman spectrum of uracil in a condensed phase is our main interest, we decided to perform our own DFT calculations, also predicting Raman intensities and mimicking solvation effects in two different ways as described by Ghomi and co-workers.[38,39] First, by the explicit addition of 2 water molecules in the calculations (Figure 1) that are capable of forming H-bonds with the two carbonyl groups and the two N−H moieties. These added water molecules can be viewed as part of a solvation shell. Second, in the context of a self-consistent reaction field (SCRF) on the basis of the Onsager theory.[37] Here the analyte is treated as a spherical cavity in the dielectric continuum of the bulk solvent. Intermolecular interaction in the solid is expected to be qualitatively similar, but stronger than that in solution.

The addition of diffuse functions is important for the theoretical treatment of anions[46] and of hydrated molecules.[43] Thus we have used the 6-31^{++}G(d,p) basis set for the calculation of the Raman spectra of neutral and deprotonated uracil.

After establishing a reliable assignment of the NRS spectrum of uracil in solution, we present the SERS spectra of uracil at different SERS substrates and at different pH values. We further discuss possible models for the interaction of uracil with the SERS substrates.

Experimental Section

Analytical grade uracil was purchased from ICN Biomedicals. All glassware was cleaned with aqua regia followed by extensive rinsing with water prior to use. Aqueous solutions were prepared using 18 MΩ high purity water. The pH was adjusted using 10 M aqueous NaOH solution.

Ag colloid was prepared according to the standard procedure of Lee and Meisel.[47] 90 mg $AgNO_3$ was dissolved in 500 mL

water and heated to boiling with extensive stirring. Ten milliliters of 1% aqueous trisodium citrate was added dropwise and the reaction mixture was boiled for another 90 min. After the solution was cooled to room temperature, the volume was adjusted with water to 500 mL. The resultant colloid was yellowish gray with an absorption maximum at 420 nm and a pH of 7.8. In this paper we will refer to this pH as neutral in comparison to an alkaline pH of 13. Colloidal suspensions were stable for several weeks and were stored in the dark at 5 °C. For SERS measurements 10 μL of colloidal suspension were mixed with 10 μL sample solutions. The final sample concentrations are mentioned in the figure captions. The samples were placed in a 3 mm diameter glass capillary for the recording of SERS.

The silver electrode was roughened in situ in a spectroelectrochemical cell consisting of a three electrode arrangement embedded in Teflon, with the silver electrode as the working electrode, a platinum counter electrode, and Ag/AgCl reference electrode. Prior to the roughening process the working electrode was prepared thoroughly using the following procedure and then placed into the spectroelectrochemical cell: (1) polish with SiC paper (P#4000) and then immerse in aqua regia for 1 min; (2) rinse with water, repolish, and rinse again with water; (3) degrease with acetone, sonicate in water for 15 min, and rinse again with water. The working electrode was roughened by applying oxidation and reduction cycles (ORC) with 0.1 M KCl (degassed) as the electrolyte. The potential was changed from −400 mV to +400 mV (relative to the standard Ag/AgCl electrode) and back to −400 mV at a sweep rate of 200 mV s^{-1}. This ORC was repeated three times. After the roughening process, the electrolyte was replaced with ca. 600 μL sample solution. SERS spectra were recorded by focusing the laser on the roughened electrode through an optical quartz window. During the measurement, the electrode potential at the working electrode was applied by a Princeton Advanced Research model 174A polarographic analyzer.

Raman and SERS spectra were recorded in a backscattering geometry on a Renishaw Raman microspectrometer system 2000 equipped with a HeNe laser (λ = 632 nm) and electrically cooled CCD detector. The laser power at the sample was 4 mW. Exposure time of the CCD was 10 seconds and 10 scans were coadded. The solvent background was removed by spectral subtraction of the solvent blank using GRAMS software.[48]

DFT calculations were carried out using Gaussian 98 software.[49] All calculations were performed by applying the hybrid of Becke's nonlocal three parameter exchange and correlation functional and the Lee−Yang−Parr correlation functional (B3LYP). The 6-31^{++}G(d,p) split valence-shell basis set augmented by d polarization functions on heavy atoms and p polarization functions on hydrogen atoms as well as diffuse functions for both hydrogen and heavy atoms was used. Solvation effects were accounted for by the explicit addition of two water molecules that could form H-bonds to the two C=O and N−H moieties of uracil, respectively. The reaction field model of solvation employed in this study is based on the Onsager model as implemented in the Gaussian 98 software. For these calculations, the SCRF=Dipole keyword was added in the input line. The parameters specified were ϵ = 78.54 (water) and a0= 3.82, 3.97, and 3.90 for neutral, N1-deprotonated and N3-deprotonated uracil, respectively, as recommended by preliminary energy calculations using the volume keyword. All wavenumber values presented in this publication are unscaled.

Results and Discussion

Normal Coordinate Analysis of Neutral Uracil. Many ab initio, perturbation theoretical, and density functional theoretical studies have been performed on the tautomerism of uracil.[35,50−55] While the different levels of theory produce different relative energies for the minor tautomers, all theoretical studies agree that the oxo-oxo form is the most stable tautomer, with all other tautomers being at least in the order of 10−25 kcal/mol less stable. Therefore, this investigation only considers the oxo−oxo tautomer.

Optimization of the geometry of neutral uracil at the B3LYP/6-31^{++}G(d,p) level of theory resulted in an essentially planar structure. All dihedral angles are smaller than 0.05°, so that, within the limits of precision, C_s symmetry can be assumed. A subsequent frequency calculation at the same level of theory produced only real frequencies, indicating that the optimized geometry represents an energy minimum. Uracil consists of 12 atoms, and its vibrational spectra, therefore, contain 30 normal modes. Twenty-one of these are in-plane in character, while the remaining nine normal modes are out-of-plane. Raman Spectroscopy is mainly suitable for the analysis of in-plane vibrations, while out-of-plane vibrations are usually weak or absent in NRS spectra.

The calculated NRS spectra of isolated and solvated uracil and the experimental NRS spectra of polycrystalline and aqueous uracil are shown in Figure 3. There is a good correlation between the NRS spectra of uracil in the different condensed phases. Because of the limited solubility of uracil in water, the aqueous solution produced a NRS spectrum with a rather poor signal-to-noise ratio with only the major peaks distinguishable from background noise. The powder spectrum shows several additional weak Raman bands.

The assignment of the calculated normal modes to the vibrational bands in the NRS spectra of uracil as a polycrystalline powder and in aqueous solution is given in Table 1 together with the description of the normal modes.

The changes in geometric parameters due to the solvation models have been discussed elsewhere.[26,36,38,56,57] The wavenumber values and assignments resulting from the two solvation models are included in Table 1 and Figure 3 with the mode numbering in Table 1 based on the predicted wavenumber values for free uracil. Uracil dihydrate vibrational modes in excess compared to those of the constituents, which have been suggested to be computational artifacts,[58] and the modes arising from the water molecules have been neglected.

Our assignment of the NRS spectrum of uracil is in good agreement with similar calculations published previously.[38,39,41−43] For a detailed discussion of the assignment refer to these earlier studies. In summary, the vibrational modes are shifted by up to 226 cm^{-1} when uracil is H-bonded to two water molecules. Even larger wavenumber shifts by up to 540 cm^{-1} were found when seven water molecules were added.[42] The wavenumber shifts caused by the dielectric continuum are negligible compared to the effect of H-bonding. Calculated wavenumber values for the uracil dihydrate are generally closer to the observed wavenumber values than those for the isolated uracil, especially in the regions >1600 cm^{-1} and <1000 cm^{-1}.

The Raman bands arising from out-of-plane ring deformations are predicted to increase in intensity when uracil is placed into a reaction field—a trend that is not observed experimentally. In fact, none of the experimental Raman bands apart from the very weak band at 828 cm^{-1} can be assigned unambiguously to a pure out-of-plane vibration. On the basis of the theoretical spectrum of free uracil, this band arises from a wagging motion

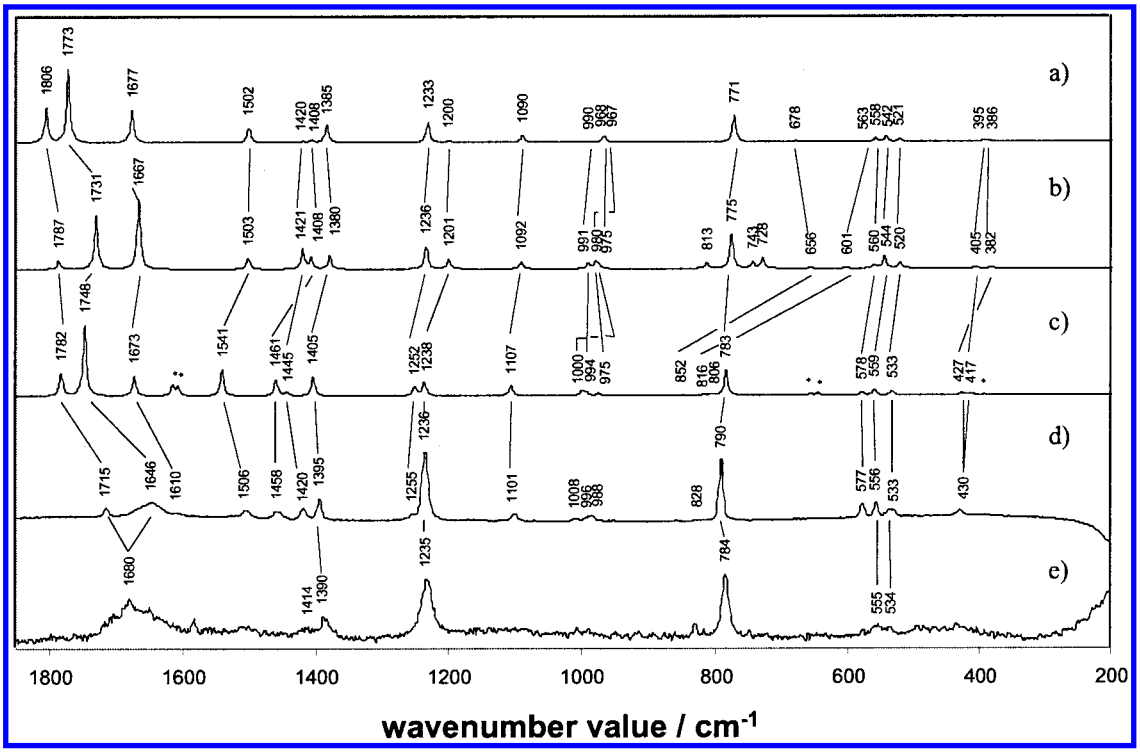

Figure 3. Theoretical Raman spectrum of uracil in the gas phase (a), in a dielectric continuum, $\epsilon = 78.5$ (b), and in a dihydrate complex (c) compared to the experimental NRS spectrum of uracil as a polycrystalline powder (d) and in saturated aqueous solution ($c \approx 3.2 \times 10^{-2}$ M) at neutral pH (e). Bands in (c) that are due to water and to intermolecular vibrations are marked with an asterisk (*).

TABLE 1: Theoretical and Experimental Wavenumber Values for the Normal Modes of Free and Solvated Uracil

	B3LYP/6-31^{++}G(d,p)					
mode	uracil dihydrate	$\epsilon = 78.5$	free uracil	NRS	plane	description
1	3422 (−226)[a]	3626 (−22)	3648	3098	in	str N1H
2	3394 (−213)	3624 (+17)	3607	3082	in	str N3H
5	1782 (−24)	1787 (−19)	1806	1715	in	str C2O (A bend N1H, N3H)
6	1748 (−25)	1731 (−42)	1773	1646	in	str C40 (A bend N3H, C5H
7	1673 (−4)	1667 (−10)	1677	1610	in	str C5C6, A bend C5H, C6H
8	1541 (+39)	1503 (+1)	1502	1506	in	bend N1H, str C6N1
9	1445 (+24)	1421 (0)	1421	1458	in	bend C6H, N1H, N3H, C5H, str C4C5
10	1461 (+53)	1408 (0)	1408	1420	in	bend N3H, N1H, str N1C2, N3C4
11	1405 (+20)	1380 (−5)	1385	1395	in	bend C6H, C5H, N1H, str N1C2−C2N3
12	1252 (+19)	1236 (+3)	1233	1236	in	A bend C5H, C6H, str N3C4−C6N1
13	1238 (+37)	1201 (0)	1201	1255	in	A bend C6H, N1H, str C2N3−N3C4
14	1107 (+17)	1092 (+2)	1090	1101	in	str C6N1, bend C5H
16	1000 (+32)	975 (+7)	968	986	in	str N1C2, N3C4, C4C5
18		813 (+2)	811	828	out	S wag C5H, C6H, def R (wag N3C4C5)
19	783 (+12)	775 (+4)	771	790	in	ring breath
22	852 (+174)	656 (−22)	678	828	out	wag N3H
23	816 (+215)	601 (+38)	563	828	out	wag N1H, C5H
24	578 (+20)	560 (+2)	558	577	in	def R (sqz groups N1C2O, C5C6N1, C2N3C4)
25	559 (+17)	544 (+2)	542	556	in	def R (sqz C2N3C4)
26	533 (+12)	520 (−1)	521	533	in	def R (sqz groups C6N1C2, N3C4C5)
27	417 (+22)	405 (+10)	395	430	out	def R (wag C5C6N1), wag N1H, N3H
28	427 (+41)	382 (−4)	386	430	in	A bend C2O, C4O

[a] Figures in parentheses correspond to shifts compared to the respective gas phase values.

of the C−H moieties (mode 18). Due to the large blue shift of the N1−H and N3−H wagging vibrations upon hydration, it is possible that these vibrations (modes 22 and 23) also contribute to this band. The corresponding very strong NIS band at 831 cm^{-1} has been assigned to the same three modes by Gaigeot et al.[45] The weak NRS band at 430 cm^{-1} may contain some contributions from the out-of-plane mode 27, but it probably derives most, if not all, of its intensity from the asymmetric bending motion of the two carbonyl groups.

DFT Calculations on Deprotonated Uracil. The assignment of the NRS of deprotonated uracil (Figure 4) is complicated by the presence of two tautomers. UV−vis and Raman spectroscopic studies have shown that in alkaline solutions ($pK_a = 9.5$) uracil anions deprotonated at N1 (tautomer **I**) and at N3 (tautomer **II**) are present in a ratio of approximately 1:1[59−61] (Figure 2). Two intense Raman bands at 797 and 787 cm^{-1} have been suggested as marker bands for tautomers **I** and **II**, respectively.[61] Our NRS spectrum of aqueous uracil at pH 13 shows an intense band at 797 cm^{-1} with a shoulder to the red (Figure 4). After deconvolution, a second band is resolved at 789 cm^{-1} (inset in Figure 4), confirming previous Raman results, which imply two tautomers are present in alkaline solution.

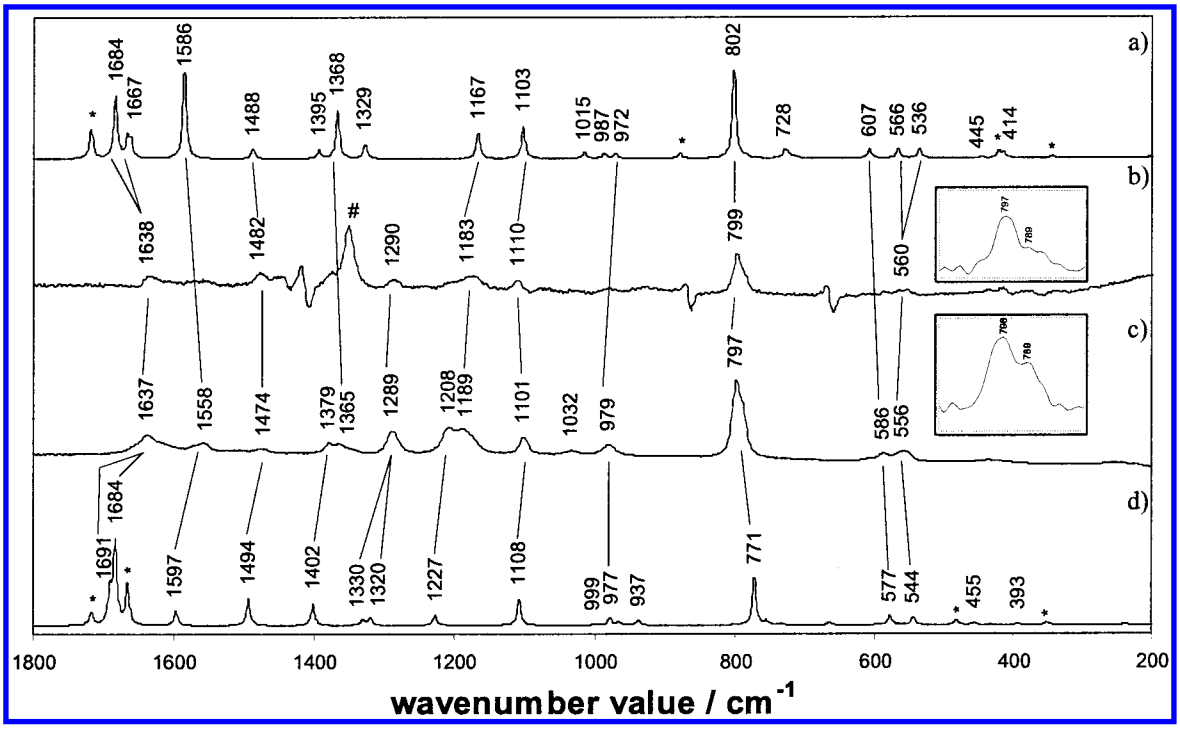

Figure 4. Theoretical Raman spectra of N1-deprotonated (a) and N3-deprotonated (d) uracil dihydrate compared to the experimental NRS spectra of saturated uracil solutions in DMF/H_2O (b) and H_2O (c) at pH = 12. Bands arising from DMF that could not completely be removed by spectral subtraction are marked "#". Bands in (a) and (d) that are due to water and to intermolecular vibrations are marked "*". The insets show the deconvolved ring breathing modes.

TABLE 2: Deprotonation Enthalpies[a] (PA) in Kcal Mol^{-1} and Relative Concentration of the Two Deprotonated Tautomers of Uracil

	6-31^{++}G(d,p)				LanL2DZ	
	ϵ = 78.5	dihydrate	combined solvation	gas phase	uracil (gas phase)	Ag-complex (gas phase)
$PA_{II} - PA_I$	4.9	9.0	0.7	13.2	14.5	−0.3
K_I/K_{II}	$3.7 \times 10^{+03}$	$1.8 \times 10^{+07}$	25.7	$2.6 \times 10^{+09}$		

[a] Including ZPE energies computed at the same level. The deprotonation energy is defined as the energy change associated with the gas-phase deprotonation reactions in Figure 2.

Full geometry optimization of the two tautomers at the B3LYP/6-31^{++}G(d,p) level shows that, in the gas phase, tautomer **I** is more stable than tautomer **II** by 13 kcal mol^{-1} (Table 2). This reflects the larger delocalization of the negative charge in tautomer **I**. As a result of its larger dipole moment, **II** is stabilized in a polar solvent like H_2O. When placed in a dielectric continuum, the energy difference between the two tautomers is reduced to 5 kcal mol^{-1}, while the complexation of 2 H_2O molecules reduces the energy differences to 9 kcal mol^{-1}. If the two solvation effects are added, the energy difference becomes a mere 0.7 kcal mol^{-1}.

Applying eq 1 to the two reactions in Figure 2, it is possible to estimate the relative concentrations of tautomers **I** and **II** in alkaline solution.

$$\Delta_R G = -RT \ln K \qquad (1)$$

The results for the gas phase and the different solvation models are presented in Table 2. In the gas-phase tautomer **I** is predicted to be 2.6×10^9 more abundant than tautomer **II**. This ratio is greatly reduced when solvation effects are taken into consideration. When the effects of both solvation models are included in the calculation in an additive manner, the ratio [**I**]/[**II**] is reduced by 8 orders of magnitude to 26. Although the two simple solvation models probably do not predict the change in energy difference between the two tautomers quantitatively, the trend indicates comparable stability of both deprotonated forms in aqueous solution. The experimentally determined acidity constants of *N*-methylated uracil are 10.0 and 9.8 for deprotonation at N1 and N3, respectively.[59] When transferring these values to the uracil monoanion, tautomer **I** would be 20% less abundant in alkaline solution than tautomer **II**.

Ilich et al.[44] reported relative stabilities at the B3LYP/6-31$^+$-G(d) level similar to our values. Despite the relative stability of the two tautomers being reversed in one of their solvation models, they did not consider N3 deprotonated uracil in their discussion of the Raman spectrum of uracil at pH 11.4 and pH 13.0. Instead, they postulated the presence of the dianion, in which both nitrogens are deprotonated. We do not agree with this assumption. Considering that pK_a for the formation of the dianion is larger than 13,[62] it is very unlikely that a solution of pH 11.4 contains the dianion in a concentration high enough to be observed in the NRS spectrum. However, at this pH there is clear evidence for the presence of a second form apart from the N1 deprotonated monoanion. Together with our theoretical calculations, this led us to assume that tautomer **II** is present in addition to tautomer **I** rather than the dianion.

It is possible to distinguish experimentally between N1 and N3 deprotonated uracil by decreasing the dielectric constant of the solvent, e.g., through the addition of dimethylformamide (DMF, ϵ = 36.7) to the aqueous solution (ϵ = 78.5).[61] Due to

TABLE 3: Assignment of the Theoretical Raman Spectra of N1- and N3-Deprotonated Uracil Dihydrate to the NRS Spectrum of Uracil at Alkaline pH and the SERS Spectra of Uracil at Neutral and Alkaline pH

			SERS				
mode	(B3LYP/)-6-31^{++}G(d,p)	NRS	Ag colloid (pH 13)	Ag colloid (pH 7)	Ag electrode (pH 7)	plane	description
I,1	3573					in	str N3H
II,1	3551					in	str N1H
I,2	3231	3108	3085	3070	3065	in	str C5H(+C6H)
II,2	3229	3108	3099	3098	3092	in	str C5H(+C6H)
II,3	3180	3024	3035			in	str C6H (−C5H)
I,3	3119	3004	3024			in	str C6H (−C5H)
II,4	1691	1637	1630	1631	1624	in	str C2O+C4O, bend N1H
I,4	1684	1637	1630	1631	1624	in	str C2O+C4O (+C5C6, bend C5H)
II,5	1684	1637	1630	1631	1624	in	str C5C6+C4O, A bend C5H, C6H
I,5	1667	1637	1630	1631	1624	in	str C2O−C4O, bend N3H
II,6	1597	1558	1580?	1570?	1597	in	str C4O−C5C6−C2O, S bend N1H, C6H
I,6	1586	1558	1536?			in	str C5C6−C6N1, bend C6H
II,7	1494	1474	1428?			in	bend N1H, C5H, C6H, str C6N1−C4C5−C2O
I,7	1488	1474	1428?			in	str N3C4−C4C5−N1C2, bend C5H
II,8	1402	1379	1407	1403	1395	in	S bend C6H, N1H, C5H
I,8	1395	1379?	1407?	1403?		in	bend C6H, N3H, C5H
I,9	1368	1365	1362	1371	1366	in	bend N3H, C5H, C6H (str C2N3)
II,9	1330	1289	1300?			in	str N1C2−C2N3+ C4C5(−C2O), bend C5H
I,10	1329	1289	1300			in	str C6N1, bend C6H, N3H, C5H
II,10	1320	1289	1278	1277	1277	in	str N3C4(−C4C5−C6N1), bend N1H, C5H, C6H
II,11	1227	1208	1225	1212	1211	in	bend N1H, C6H, C5H, str C6N1
I,11	1167	1189	1217	1212?		in	str N1C2−C2N3+N3C4− C4C5, bend C6H
II,12	1108	1101	1107	1100	1083	in	bend C5H, str C5C6+C6N1
I,12	1103	1101	1107	1100	1083?	in	bend C5H (bend C6H, str C5C6+C6N1)
I,13	1015	1032	1047	1037	1048	in	def R (str N3C4+C4C5)
II,13	999	979	1010		1005	in	str N1C2−C4C5, bend C6H
I,14	987	979	1010		1005	out	wag C6H
II,14	977	979	1010		1005	in	def R (sqz groups C5C6N1, N3C4C5)
I,15	972	979	1010		1005	in	def R (sqz group N1C2N3)
II,15	937	979	1010		1005	out	A wag C5H, C6H
II,16	806			866?		out	def R (tors C4C5), S wag C5H, C6H
I,16	802	797	807			in	ring breath
I,17	788					out	def R (tors N1C2), wag C5H
I,18	783					out	def R (wag C2N3C4), wag C5H
II,17	773					out	wag C5H, C6H, N1H, def R (wag C4C5C6)
II,18	771	789	801	801	800	in	ring breath
II,19	764				759	out	def R (wag N1C2N3)
II,20	754		737?		732	out	def R (wag N1C2N3)
I,19	728		737?			out	wag C5H
I,20	723					out	wag N3H
II,21	664		692?			out	wag N1H (C6H, C5H)
I,21	607	sh?	645			in	def R (sqz group C2N3C4, O4C4C5 N1C2O)
II,22	593	586?	603?	596?	600?	in	def R (sqz groups N3C2O, N3C4O)
II,23	577	586	603	596	600	in	def R (sqz groups C2N3C4, C5C6N1)
I,22	566	556	560	561	560	in	def R (sqz groups C2N3C4, C5C6N1)
II,24	544	556	560?	561	560	in	def R (sqz groups N3C4C5, C6N1C2)
I,23	536	556	560	526?	560	in	def R (sqz groups N3C4C5,C6N1C2)
II,25	455		456?			in	bend C2O, C4O
I,24	445					out	def R (wag C5C6N1), wag N3H
I,25	414	434	456?	436	438	in	bend C2O, C4O
II,26	393				393	out	def R (wag C5C6N1, C2N3C4) wag N1H
II,27	196					out	def R (wag C2N3C4) wag N1H, C2O, C4O
I,26	192					out	def R (tors C5C6N1) wag C2O, C4O
I,27	167					out	def R (wag C2N3C4) wag C2O, C4O
II,28	128					out	def R (tors C5C6N1) wag C2O, C4O

its smaller dipole moment, tautomer **I** is favored in a 1:1 mixture of DMF and H_2O compared to a purely aqueous solution. Consequently, those bands in the NRS spectrum of uracil that are considerably reduced in intensity after the addition of DMF can be assigned to tautomer **II**, while bands originating from vibrations of tautomer **I** increase in relative intensity (Figure 4). This method is limited to relatively intense NRS bands, since the decreased solubility in DMF/H_2O only allowed the recording of a NRS spectrum with a rather poor signal-to-noise ratio. Interference of NRS bands from DMF further limited the applicability of this method. Despite these limitations, by combining the theoretical and experimental results the bands at 1287 cm^{-1}, 1205, 789, and 586 cm^{-1} can be assigned to vibrations of tautomer **II** with a high degree of certainty, while vibrations of tautomer **I** give rise to NRS bands at 556, 797, and 1189 cm^{-1}. The complete assignment of the NRS spectrum of uracil at alkaline pH is presented in Table 3 and Figure 4. Only the results of the DFT calculations on the uracil anion dihydrate complexes are reported here. The respective results of the calculations on the anions in the gas phase and in a self-consistent reaction field can be obtained from the authors on request.

From the NRS spectrum of uracil in alkaline solution, it is not possible to determine exactly the ratio of tautomers **I** and

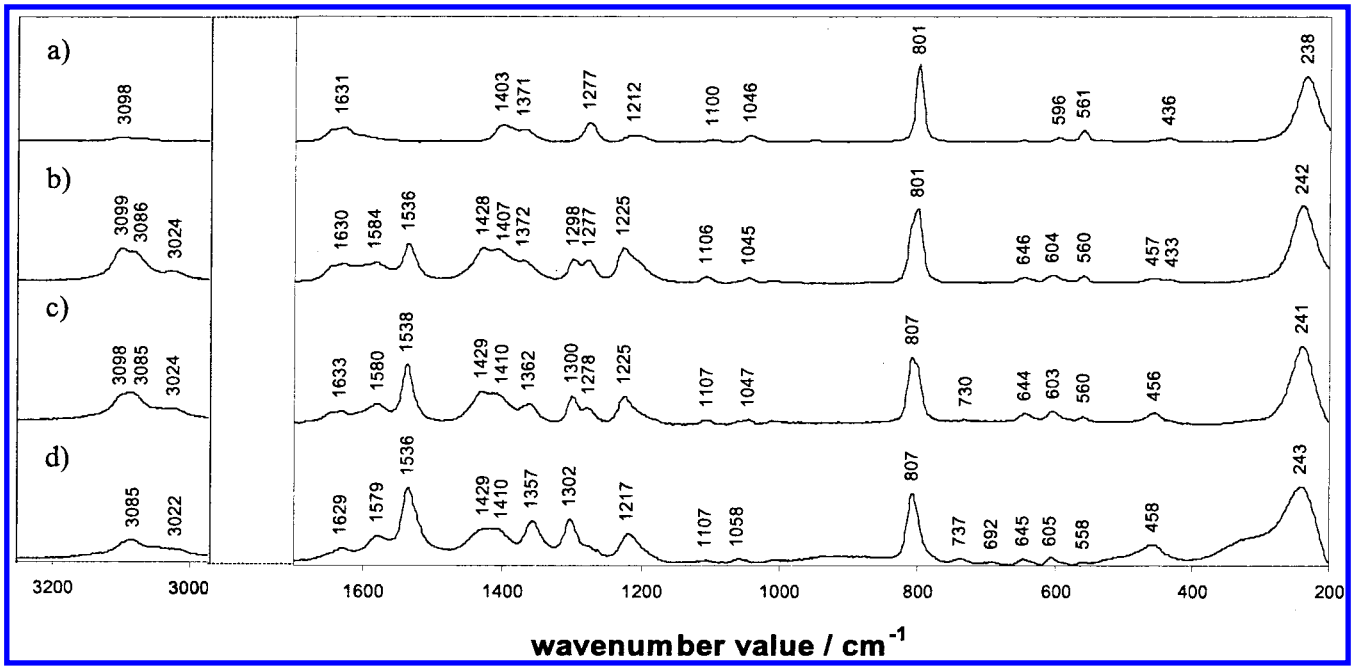

Figure 5. SERS spectrum of uracil in a silver sol at pH 7.8 (10^{-5} M, a) and pH 13 at a concentration of 10^{-2} M (b), 10^{-4} M (c), and 10^{-6} M (d).

II, since the spectra of the pure tautomers are not available. However, from the relative intensity of the bands at 797 and 789 cm^{-1} and considering that the absolute Raman intensity of the latter is predicted to be two-thirds of the former, the ratio can be estimated to be 53:47. This value is consistent with previous UV−vis and Raman results.[59−61]

SERS of Uracil in a Silver Sol. The SERS spectra of uracil in silver colloid at neutral and alkaline pH are shown in Figure 5. The SERS spectrum at neutral pH shows much better correlation with the NRS spectrum of uracil in alkaline solution (Figure 4) than with the NRS spectrum at neutral pH (Figure 3). For example, the SERS bands at 1403, 1277, 1212 , 1037, 596, and 561 cm^{-1} correspond to the NRS bands of deprotonated uracil at 1379, 1289, 1208/1189, 1032, 586, and 556 cm^{-1}, respectively. Corresponding bands for most of these SERS bands cannot be identified in the NRS spectrum of neutral uracil (Figure 3). To interpret the SERS spectrum of uracil at neutral pH, the SERS spectrum has also been measured at alkaline pH. All bands present in the SERS spectrum at neutral pH are also observed at higher pH, providing further evidence that uracil adsorbs to the silver surface in its deprotonated form even at neutral pH. At alkaline pH, however, several new bands appear in the SERS spectrum that are not present at neutral pH. The most likely explanation for the additional bands at high pH is the coexistence of both deprotonated tautomers, while only one tautomer may be present at neutral pH.

The most intense band in the SERS spectrum of uracil at alkaline pH (Figure 5c) is located at 807 cm^{-1} with a shoulder at about 801 cm^{-1}. These two SERS bands correspond to the NRS bands at 798 and 789 cm^{-1}, which have been assigned to the ring breathing modes of tautomers **I** and **II**, respectively (Table 3). In the SERS spectrum at neutral pH, only the band at 801 cm^{-1} appears without a detectable shoulder indicating that only tautomer **II** is present. The occurrence of a SERS band at 1277 cm-^{1} at neutral pH supports this conclusion, as it corresponds to the NRS band at 1289 cm^{-1}, which has been assigned exclusively to a normal mode of tautomer **II**. The strong band at 1538 cm^{-1} in the SERS spectrum at alkaline pH could, in principle, be assigned to modes **I**,6 or **II**,7. However, its total absence at neutral pH together with our previous conclusion, that at neutral pH only tautomer **II** adsorbs to the colloid, strongly suggests that it arises exclusively from mode **I**,6. Consequently, it can be used as a marker band for tautomer **I** in the adsorbed state, in addition to the ring breathing mode at 807 cm^{-1}. The large SERS intensity of the band at 1538 cm^{-1} can be explained on the basis of the surface selection rules[17,27] (vide supra). It arises from a vibration dominated by the stretching of the C5═C6 bond. When the uracil anion interacts with the silver surface via N1 and adopts an upright orientation, this bond is exactly perpendicular to the surface. For such a case, the surface selection rules predict particularly large enhancement, which is in agreement with our experimental results.

In summary, only the pK_a value for deprotonation at N3, but not at N1, seems to be lowered sufficiently in the presence of Ag colloid to generate uracil anions at pH 7.8 that can interact with the positively charged Ag surface via the negatively charged nitrogen. Positive charges on the silver colloid surface obviously lower the pK_a value of uracil by Coulombic stabilization of the deprotonated anion. This stabilization is higher for tautomer **II** compared to tautomer **I** due to less delocalization of the negative charge and a higher dipole moment, thus rendering the former to be the dominant tautomer in the adsorbed state. On the other hand, at alkaline pH N1- and N3-deprotonated uracil is present in the solution and both tautomers adsorb to the colloidal surface. The model we propose for the interaction of uracil with the Ag colloid at different pH is illustrated in Figure 6.

To test our hypothesis, DFT calculations have been performed on tautomers **I** and **II** of deprotonated uracil and their complexes with a silver cation. The 6-31^{++}G(d,p) basis set generally used in this work is only applicable to elements lighter than Cl. The heavy Ag^+ ion, therefore, required the use of the LanL2DZ basis set implemented in the Gaussian software. Results of calculations using this basis set and the B3LYP DFT functionals are included in Table 2. Tautomer **I** is predicted to be more stable than tautomer **II** by 14.5 kcal mol^{-1}, a value slightly larger than the corresponding energy difference when the 6-31^{++}G(d,p) basis set is used. For the respective Ag-complexes, the energy levels are reversed. Tautomer **II** becomes more stable than

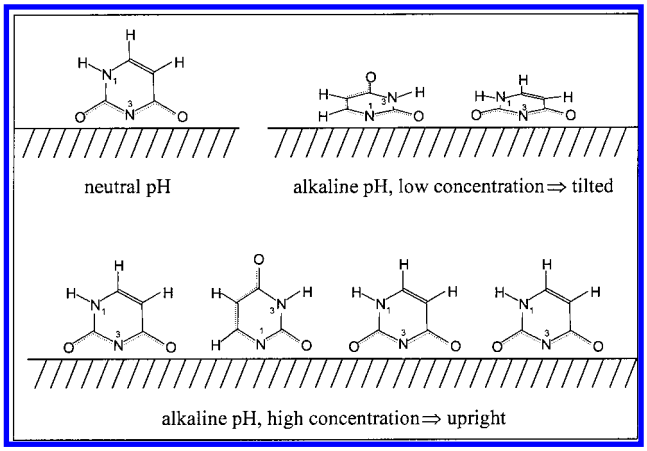

Figure 6. Proposed models for the orientation of uracil on the Ag surface.

tautomer **I** by 0.3 kcal mol^{-1}. While the energy gap between the two complexes is rather small, our calculations, nevertheless, simulated the observed trend.

In contrast to the SERS spectrum at neutral pH, the SERS spectrum at alkaline pH is concentration dependent in the range between 10^{-2} and 10^{-6} M. There are two different effects that may manifest themselves in the SERS spectra at different concentrations: a change in orientation of the adsorbate on the metal surface and a change in the ratio of tautomers **I** and **II**. To derive adsorbate orientations on the substrate, surface specific surface selection rules have been developed on the basis of the electromagnetic enhancement model.[17] They quote that those normal modes with a change in polarizability perpendicular to the surface are particularly enhanced. As suggested by Suh and Moskovits,[24] the CH stretching bands in the high wavenumber region can be used as marker bands for an upright orientation of the adsorbate. For a flat orientation the surface selection rules would predict no substantial enhancement of these bands at about 3090 and 3025 cm^{-1}, since in that case the corresponding vibrations would lead to only minimal change in polarizability perpendicular to the metal surface. A decrease in intensity of these bands with decreasing concentration suggests a reorientation of the adsorbate from upright to tilted and almost flat. This interpretation is also supported by additional SERS bands at 692 and 732 cm^{-1} at the lowest concentration ($c = 10^{-6}$ M). These bands can, with a high degree of certainty, be assigned to out-of-plane modes, because the closest in-plane modes are predicted at 607 and 771 cm^{-1}, and these modes are unlikely to be shifted by 40 cm^{-1} or more upon adsorption. According to the surface selection rules,[17] out-of-plane vibrations are expected in the SERS spectrum only when the analyte adopts a flat or at least tilted orientation. The increased intensity of the band at 457 cm^{-1} may also be a result of this reorientation from upright to tilted, because it probably contains contributions from out-of-plane vibrations as well as in-plane vibrations.

Other spectral changes with decreasing concentration include an increase in intensity of the SERS band at 1536 cm^{-1}, a shift of the band at 1372 cm^{-1} to 1357 cm^{-1} and a concurrent increase in intensity, an intensity decrease of the band at 1277 cm^{-1}, and shift of the ring breathing mode from 801 cm^{-1} with a shoulder to the blue to 807 cm^{-1} with a shoulder to the red. All these changes are consistent with a shift of the position of the equilibrium between tautomers **I** and **II** in favor of tautomer **I**. This concentration dependence can be explained by the adsorbate coverage on the surface.

At high concentrations, adsorbate crowding leads to the adoption of an upright orientation and severe competition between the two tautomers for adsorption spots. The SERS spectrum is dominated by bands attributed to tautomer **II**. This is in agreement with the SERS experiment at neutral pH and the theoretical calculations, which had shown that tautomer **II** has greater affinity to the Ag surface than tautomer **I**. When the concentration is decreased, particularly when it is decreased below the monolayer threshold, tautomer **II** occupies less adsorption spots and more spots become available for adsorption of tautomer **I**. This trend is manifested in the SERS spectrum: The tautomer **I** marker bands at 1536 and 807 cm^{-1} increase in intensity. At the same time the increased available space per adsorbed molecule allows the adoption of a more tilted or almost flat orientation reflected in an intensity increase of the out-of-plane vibrations and an intensity decrease of the C−H stretching vibrations above 3000 cm^{-1}.

Simple geometric calculations can be performed, assuming that (1) the colloidal particles are isolated spheres with a diameter of 30 nm, (2) every molecule occupies a circular space with a radius of 3.9 Å (a0 value for tautomer **II** obtained from DFT calculations using the volume keyword), (3) the adsorbates adopt a flat orientation on the surface, and (4) a monolayer is completed before the onset of multilayers. This way the concentration needed for the completion of a monolayer is estimated at 3.8×10^{-6} M. Although this estimation is fairly crude, it indicates that the monolayer threshold is probably within the investigated concentration range.

Comparison with previously published SERS spectra leads to some interesting observations. Our SERS spectrum at alkaline pH (intermediate to low concentration) is very similar to the SERS spectrum reported by Oh et al. and Suh and Moskovits in a borohydride reduced silver sol at neutral pH.[23,24] When excess borohydride was added to the neutral silver sol, Oh et al.[23] obtained a SERS spectrum basically identical to our SERS spectrum at neutral pH. They attributed the spectral changes to a molecular reorientation at the silver surface as a result of a decreased surface potential. Following interpretations by Brabec et al.,[22] Oh et al.[23] concluded flat orientation of uracil on the silver surface. Brabec et al.,[22] however, had transferred the results of an electrochemical study of uracil adsorbed on a mercury electrode to the corresponding silver system and postulated that uracil lay flat on the silver electrode surface at an electrode potential of −0.1 to −0.6 V vs SCE. It is important to stress that there is no spectral evidence for this conclusion. We believe that a shift in the relative abundances of the two possible deprotonated tautomers is more likely to be responsible for the observed spectral changes than a molecular reorientation.

The silver colloid employed in this study was prepared in a different way than in the studies mentioned above. Instead of borohydride, citrate was used as a reduction reagent, which served the additional function of stabilizing the produced colloid. Obviously, citrate modified the colloid in a similar way to excess borohydride, possibly by reducing the surface potential.

SERS of Uracil at a Silver Electrode. Although the direct comparison of SERS spectra on colloids and metal electrodes has limitations, it is the only methodology available to us for the exploration of changes due to the effect of varying applied potential. Hence, to elucidate the impact of the surface potential on the adsorption behavior of uracil on silver surfaces, we recorded the SERS spectra of uracil at neutral pH on an electrochemically roughened silver electrode (Figure 7). At open circuit, viz. 0 V vs saturated Ag/AgCl reference electrode, the SERS spectrum resembles the SERS spectrum at neutral pH in a citrate reduced silver sol, indicating similar adsorbate−adsorbens interaction in both systems. No evidence was found

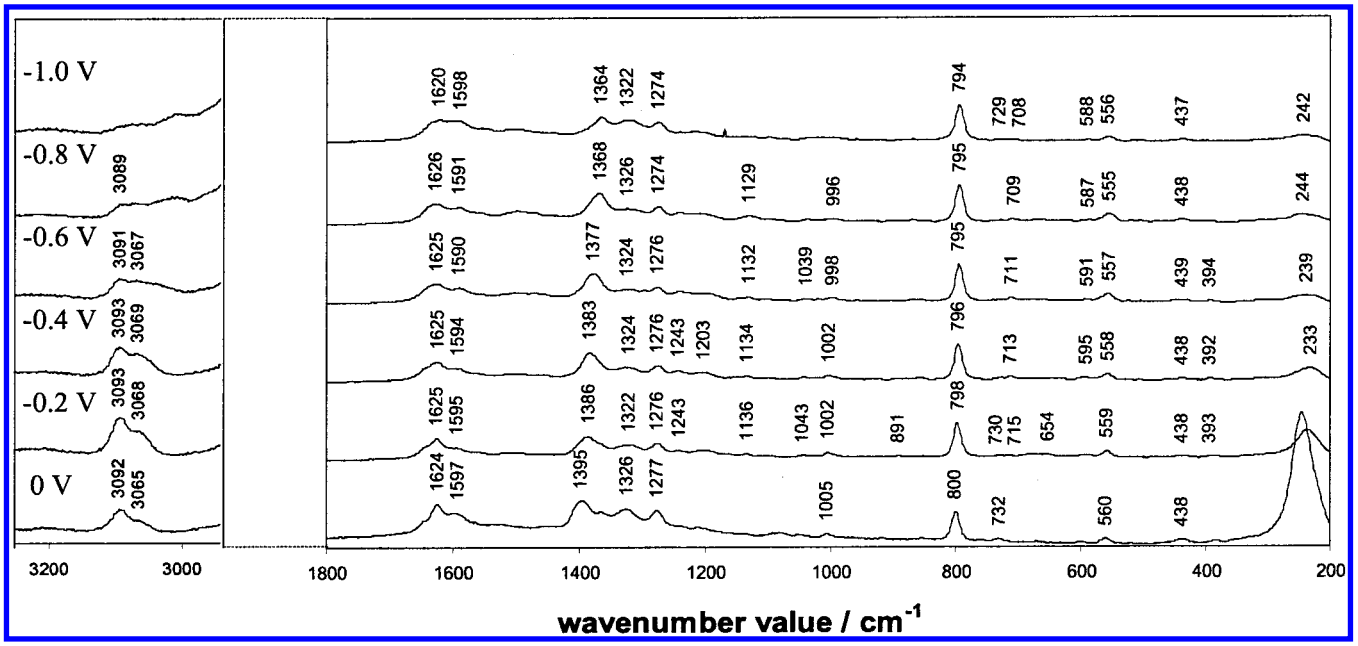

Figure 7. SERS spectrum of 10^{-4} M uracil at a silver electrode as a function of the electrode potential. Raman intensities in the high wavenumber region have been multiplied by a factor of 10 for better visualization.

for the adsorption of N1 deprotonated uracil. On the contrary, the absence of a SERS band at 1536 cm^{-1} and the position of the ring breathing mode at 800 cm^{-1} without any shoulder to the blue leads us to the assumption that the N3-deprotonated tautomer is the only adsorbed species in the electrode system as well as in the silver sol.

Despite the large resemblance of the SERS spectra of uracil at the two surface substrates, some small differences do exist. For example, the carbonyl stretching band located at 1631 cm^{-1} in the silver sol is shifted to 1624 cm^{-1} at the silver electrode. This slight red shift may be the result of a larger contribution of one or both of the carbonyl groups adjacent to N3 to the interaction with the metal surface. The weak SERS band at 732 cm^{-1}, which is not present in the colloid spectrum, is most likely assigned to an out-of-plane vibration and may, therefore, be indicative of a more tilted rather than upright orientation relative to the metal surface. On the other hand, the very intense ring breathing mode and the presence of the C−H stretching mode at about 3090 cm^{-1} excludes the adoption of a totally flat orientation.

Most of the SERS bands are sensitive to the surface potential. The more obvious spectral changes upon decreasing the applied potential from 0 V to −1 V include the red shift of the bands at 1395, 1048, 1005, 800, 600, and 560 cm^{-1} to 1364, 1036, 994, 794, 588, and 556 cm^{-1}, respectively. The gradual nature of these changes makes it unlikely that they are the result of a molecular reorientation or of the adsorption of a different tautomer. Rather, they can be explained by an inductive effect of the increasingly negative electrode. None of the tautomer **I** marker bands is observed at any of the applied surface potentials. According to our assignments (Table 3) the SERS bands at 732 cm^{-1}, 709, 519, and 509 cm^{-1} arise partially or completely from out-of-plane vibrations. Since these bands do not follow a uniform trend upon variation of the electrode potential, no conclusion can be inferred with regard to molecular reorientation.

An analogous red shift of the ring breathing mode upon decreasing surface potential has been observed in the SERS spectrum of adenine[63] (800−794 cm^{-1} for uracil and 732−728 cm^{-1} for adenine) and has been used to estimate the surface potential of the silver colloids used in the SERS experiments. The wavenumber value of 801 cm^{-1} in the colloidal SERS spectrum of uracil at neutral pH indicates a potential of 0 V (or slightly more positive) vs Ag/AgCl at the colloidal surface.

Conclusion

The NRS spectra of neutral and deprotonated uracil have been predicted by DFT calculations at the B3LYP/6-31G^{++}(d,p) level, also taking into consideration solvation effects. These calculations, together with experimental NRS spectra in solvents with different dielectric constants, allowed the identification of two different deprotonated tautomers at alkaline pH: N1- and N3-deprotonated uracil. The assignment of the Raman bands to the two tautomers was helpful in the interpretation of the SERS spectra recorded at different silver surfaces.

The result of our SERS spectra of uracil on a silver electrode at varying applied potential is not consistent with the assumption by Oh et al.[23] that uracil undergoes a reorientation from standing upright to lying flat on the silver surface as the surface charge is made more negative. We rather believe the different SERS spectra obtained when different silver colloids are used may be due to the presence of two deprotonated uracil tautomers in the case of the standard borohydride colloid, and of only one tautomer, viz. tautomer **II**, in the case of the citrate colloid and the colloid with excess borohydride. At alkaline pH on a citrate reduced colloid both tautomers are present. Spectral changes upon variation of the concentration can be explained in terms of coverage of adsorption sites and molecular reorientation.

References and Notes

(1) Sanchez-Cortes, S.; Garcia-Ramos, J. V. *Langmuir* **2000**, *16*, 764.
(2) Sanchez-Cortes, S.; Garcia-Ramos, J. V. *Vib. Spectrosc.* **1993**, *4*, 185.
(3) Sanchez-Cortes, S.; Garcia-Ramos, J. V. *J. Raman Spectrosc.* **1992**, *23*, 61.
(4) Camafeita, L. E.; Sanchez-Cortes, S.; Garcia-Ramos, J. V. *J. Raman Spectrosc.* **1996**, *27*, 533.
(5) Otto, C.; Tweel, T. J. J. v. d.; Mul, F. F. M. d.; Greve, J. *J. Raman Spectrosc.* **1986**, *17*, 289.
(6) Otto, C.; Mul, F. F. M. d.; Huizinga, A.; Greve, J. *J. Phys. Chem.* **1988**, *92*, 1239.

(7) Kim, S. K.; Joo, T. H.; Suh, S. W.; Kim, M. S. *J. Raman Spectrosc.* **1986**, *17*, 381.
(8) Koglin, E.; Sequaris, J. M.; Valenta, P. *J. Mol. Struct.* **1980**, *60*, 421.
(9) Koglin, E.; Sequaris, J.-M.; Fritz, J.-C.; Valenta, P. *J. Mol. Struct.* **1984**, *114*, 219.ews
(10) Moskovits, M. *Rev. Mod. Phys.* **1985**, *57*, 783.
(11) Campion, A.; Kambhampati, P. *Chem. Soc. Rev.* **1998**, *27*, 241.
(12) Otto, A.; Billmann, J.; Eickmans, J.; Ertuerk, U.; Pettenkofer, C. *Surf. Sci.* **1984**, *138*, 319.
(13) Otto, A.; Mrozek, I.; Grabhorn, H.; Akemann, W. *J. Phys.: Condens. Matter* **1992**, *4*, 1143.
(14) Kneipp, K.; Wang, Y.; Kneipp, H.; Itzkan, I.; Dasari, R. R.; Feld, M. S. *Phys. Rev. Lett.* **1996**, *76*, 2444.
(15) Kneipp, K.; Wang, Y.; Kneipp, H.; Perelman, L. T.; Itzkan, I.; Dasari, R. R.; Feld, M. S. *Phys. Rev. Lett.* **1997**, *78*, 1667.
(16) Nie, S.; Emory, S. R. *Science* **1997**, *275*, 1102.
(17) Creighton, J. A. *Surf. Sci.e* **1983**, *124*, 209.
(18) Creighton, J. A. In *Spectroscopy of Surfaces*; Clark, R. J. H., Hester, R. E., Eds.; Wiley: New York, 1988; pp 37.
(19) Greslion, S.; Aigouy, L.; Boccara, A. C.; Rivoal, J. C.; Quelin, X.; Desmarest, C.; Gadenne, P.; Shubin, V. A.; Sarychev, A. K.; Shalaev, V. M. *Phys. Rev. Lett.* **1999**, *82*, 4520.
(20) Markel, V. A.; Shalaev, V. M.; Zhang, P.; Huynh, W.; Tay, L.; Haslett, T. L.; Moskovits, M. *Phys. Rev. B* **1999**, *59*, 10903.
(21) Giese, B.; McNaughton, D. *J. Phys. Chem. B* **2001**, in press.
(22) Brabec, V.; Niki, K. *Collect. Czech. Chem. Commun.* **1986**, *51*, 167.
(23) Oh, W. S.; Suh, S. W.; Kim, M. S. *J. Raman Spectrosc.* **1988**, *19*, 261.
(24) Suh, J. S.; Moskovits, M. *J. Am. Chem. Soc.* **1986**, *108*, 4711.
(25) Torres, E. L.; Winefordner, J. D. *Anal. Chem.* **1987**, *59*, 1626.
(26) Xue, Y.; Pan, S. *Fenzi Kexue Xuebao* **1999**, *15*, 68.
(27) Moskovits, M.; Suh, J. S. *J. Phys. Chem.* **1984**, *88*, 5526.
(28) Moskovits, M.; Suh, J. S. *J. Phys. Chem.* **1984**, *88*, 1293.
(29) Nishimura, Y.; Tsuboi, M.; Kato, S.; Morokuma, K. *J. Am. Chem. Soc.* **1981**, *103*, 1354.
(30) Florian, J.; Hrouda, V. *Spectrochim. Acta* **1993**, *49A*, 921.
(31) Harsanyi, L.; Csaszar, P.; Csaszar, A.; Boggs, J. E. *Int. J. Quantum Chem.* **1986**, *29*, 799.
(32) Person, W. B.; Szczepaniak, K. Calculated and Experimental Vibrational Spectra and Force Fields for Isolated Pyrimidine Bases. In *Vibrational Spectra and Structure*; Durig, J. R., Ed.; M. Dekker: New York, 1992; Vol. 20, p 239.
(33) Rush, III, T.; Peticolas, W. L. *J. Phys. Chem.* **1995**, *99*, 14647.
(34) Les, A.; Adamowicz, L.; Nowak, M. J.; Lapinski, L. *Spectrochim. Acta* **1992**, *48A*, 1385.
(35) Estrin, D. A.; Paglieri, L.; Corongiu, G. *J. Phys. Chem.* **1994**, *98*, 5653.
(36) Paglieri, L.; Corongiu, G.; Estrin, D. A. *Int. J. Quantum Chem.* **1995**, *56*, 615.
(37) Onsager, L. *J. Am. Chem. Soc.* **1936**, *58*, 1486.
(38) Aamouche, A.; Berthier, G.; Cadioli, B.; Gallinella, E.; Ghomi, M. *J. Mol. Struct. (THEOCHEM)* **1998**, *426*, 307.
(39) Ghomi, M.; Aamouche, A.; Cadioli, B.; Berthier, G.; Grajcar, L.; Baron, M. H. *J. Mol. Struct.* **1997**, *410*−*411*, 323.
(40) Bencivenni, L.; Ramondo, F.; Pieretti, A.; Sanna, N. *J. Chem. Soc., Perkin Trans. 2* **2000**, 1685.
(41) van Mourik, T. *Phys. Chem. Chem. Phys.* **2001**, *3*, 2886.
(42) Gaigeot, M.-P.; Kadri, C.; Ghomi, M. *J. Mol. Struct.* **2001**, *565*−*566*, 469.
(43) Gaigeot, M.-P.; M., G. *J. Phys. Chem. B* **2001**, *105*, 5007.
(44) Ilich, P.; Hemann, C. F.; Hille, R. *J. Phys. Chem. B* **1997**, *101*, 10923−10938.
(45) Gaigeot, M.-P.; Leulliot, N.; Ghomi, M.; Jobic, H.; Coulombeau, C.; Bouloussa, O. *Chem. Phys.* **2000**, *261*, 217.
(46) Foresman, J. B.; Frisch, E. *Exploring Chemistry with Electronic Structure Methods*, 2nd ed.; Gaussian, Inc.: Pitsburgh, PA, 1996.
(47) Lee, P. C.; Meisel, D. *J. Phys. Chem.* **1982**, *86*, 3391.
(48) G. I. Corporation. GRAMS/32, 4.14 ed.; Salem, NH, 3079, 1991.
(49) Frisch, M. J.; Trucks, G. W.; Schlegel, H. B.; Scuseria, G. E.; Robb, M. A.; Cheeseman, J. R.; Zakrzewski, V. G.; Montgomery, J. A.; Stratmann, R. E.; Burant, J. C.; Dapprich, S.; Millam, J. M.; Daniels, A. D.; Kudin, K. N.; Strain, M. C.; Farkas, O.; Tomasi, J.; Barone, V.; Cossi, M.; Cammi, R.; Mennucci, B.; Pomelli, C.; Adamo, C.; Clifford, S.; Ochterski, J.; Petersson, G. A.; Ayala, P. Y.; Cui, Q.; Morokuma, K.; Malick, D. K.; Rabuck, A. D.; Raghavachari, K.; Foresman, J. B.; Ciolowski, J.; Ortiz, J. V.; Stefanov, B. B.; Liu, G.; Liashenko, A.; Piskorz, P.; Komaromi, I.; Gomperts, R.; Martin, R. L.; Fox, D. J.; Keith, T.; Al-Laham, M. A.; Peng, C. Y.; Nanayakkara, A.; Gonzalez, C.; Challacombe, M.; Gill, P. M. W.; Johnson, B. G.; Chen, W.; Wong, M. W.; Andres, J. L.; Head-Gordon, M.; Replogle, E. S.; Pople, J. A. *Gaussian 98* Rev. A6; Gaussian, Inc.: Pittsburgh, PA, 1998.
(50) Gould, I. R.; Hillier, I. H. *J. Chem. Soc., Perkin Trans. 2* **1990**, 329.
(51) Leszczynski, J. *Int. J. Quantum Chem. Quantum Biol. Symp.* **1991**, *18*, 9.
(52) Leszczynski, J. *J. Phys. Chem.* **1992**, *93*, 2554.
(53) Les, A.; Adamowicz, I. *J. Phys. Chem.* **1992**, *93*, 1649.
(54) Boughton, J. W.; Pulay, P. *Int. J. Quantum Chem.* **1993**, *47*, 49.
(55) Tian, S. X.; Zhang, C. F.; Zhang, Z. J.; Chen, X. J.; Xu, K. Z. *Chem. Phys.* **1999**, *242*, 217.
(56) Chandra, A. K.; Nguyen, M. T.; Zeegers-Huyskens, T. *J. Phys. Chem. A* **1998**, *102*, 6010.
(57) Van Mourik, T.; Price, S. L.; Clary, D. C. *J. Phys. Chem. A* **1999**, *103*, 1611.
(58) Williams, R. W.; Cheh, J. L.; Lowrey, A. H.; Weir, A. F. *J. Phys. Chem.* **1995**, *99*, 5299.
(59) Nakanishi, K.; Suzuki, N.; Yamazaki, F. *Bull. Chem. Soc. Jpn* **1961**, *34*, 53.
(60) Shapiro, R.; Kang, S. *Biochim. Biophys. Acta* **1971**, *232*, 1.
(61) Lippert, B. *J. Raman Spectrosc.* **1979**, *8*, 274.
(62) Dawson, R. M. C.; Elliot, D. C.; Elliot, W. H.; Jones, K. M. In *Data for Biochemical Research*; Oxford Science Publications: Clarendon, Oxford, U.K., 1990; p 98.
(63) Otto, C.; Lucassen, G. W.; Greve, J. In *Proceedings XIIth International Conference on Raman Spectroscopy*; Durig, J. R., Sullivan, J. F., Ed.; Wiley: New York, 1990; p 326.